

# DESIGNING OF SVPWM DRIVER FOR INDUCTION MOTOR DRIVEN EV

G.Syed Zabiyyullah<sup>1</sup>, Prabhakaran.R<sup>2</sup>, R.Gunasekaran<sup>3</sup>

<sup>2</sup>(PG Student, Excel college of Engineering and Technology, Komarapalayam)

<sup>1,3</sup>(Assistant Professor/EEE, Excel college of Engineering and Technology, Komarapalayam)

## Abstract:

This project cares with design concerns and trade-offs concerned within the power electronics development for lightweight electrical vehicles. A review of propulsion system design, power conversion structure and control is presented. A three-phase squirrel-cage induction motor is used as propulsion system for an electric scooter. The motor is controlled at different operating conditions by means of a space vector control using a low cost controller board developed for light electric vehicles used in local areas. Experimental results show that the proposed digital controller is able to follow the reference speed with a suitable dynamics for the electric scooter.

*Keywords — Digital Controller, Electric Scooter, Space Vector Control, Speed.*

## I.INTRODUCTION

Environmental quality of cities is an emerging issue. The ever increasing traffic volume has produced high levels of carbon dioxide emissions from the conventional gasoline and diesel-fuelled vehicles, which will contribute to a substantial increase of pollution in the major cities all over the world, causing heavy consequences to the communities. It has been recognized that electric vehicles are the only viable solution in order to reduced air pollution, in particular, in large urban areas. However, electrical vehicles have serious disadvantages because of the limitation on cruising range imposed by weight, capacity of the batteries and long recharging time. Electric scooters are a step towards the solution for the environmental problems and traffic congestion created by cars. Moreover, electric scooters are competitive when devoted to urban mobility where it is not necessary an extended driving range. Therefore, there search and development of electric scooters in order to reduce air pollution and environmental damage becomes relevant. In addition, if those disadvantages can be overcome,

motorcycles customers will be motivated to purchase electric motorcycles in the near future. Therefore, our objective in this project is to establish an appropriate platform for the study of electric motor cycles, and then to design a low cost controller for the achievements of the desired control objectives. Pulse width modulation (PWM) has been studied extensively during the past decades.

Many different PWM methods have been developed to achieve the following aims: wide linear modulation range; less switching loss; less total harmonic distortion (THD) in the spectrum of switching waveform; and easy implementation and less computation time.

For a long period, carrier-based PWM methods were widely used in most applications. The earliest modulation signals for carrier-based PWM are sinusoidal. The use of an injected zero-sequence signal for a three-phase inverter initiated the research on non sinusoidal carrier-based PWM. Different zero-sequence signals lead to different non sinusoidal PWM modulators. Compared with sinusoidal three-phase PWM, non sinusoidal three-phase PWM can extend the linear modulation range for line-

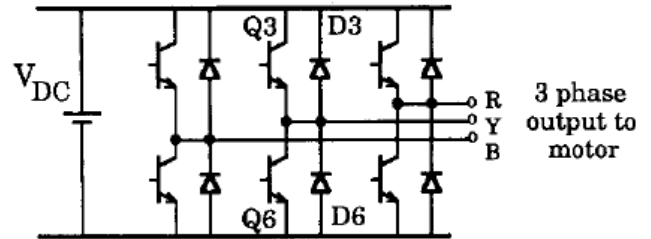
to-line voltages. With the development of microprocessors, space-vector modulation has become one of the most important PWM methods for three-phase converters. It uses the space-vector concept to compute the duty cycle of the switches. It is simply the digital implementation of PWM modulators. The comprehensive relation of the two PWM methods provides a platform not only to transform from one to another, but also to develop different performance PWM modulators. Therefore, many attempts have been made to unite the two types of PWM methods.

The relationship between space vectors and fundamental modulation signals was derived. Reference suggested the relationship between common-node voltage (zero-sequence voltage) and the space vectors on the basis of a three-phase inverter with a symmetrical Y-connected load. However, the dependence on the load hinders the universal significance of its drawn conclusions. This project aims to reveal the comprehensive relationship between space-vector modulation and carrier-based PWM. The relationship between modulation signals and voltage vectors, the relationship between zero-sequence signal and space vectors, the relationship between the modulation signals and the vector sectors, the relationship between the sequence of space vectors and the type of carrier, and the relationship between the distribution of zero vectors and different carrier-based PWM modulators are systematically investigated without dependence on the load type. Furthermore, the implementations of these two PWM methods in the feedback closed-loop converter are discussed with corresponding solutions. Simulation results are provided to validate the drawn conclusions.

## II. SPACE VECTOR MODULATION

Conceptually a set of three phase waveforms can be represented by a single rotating vector - often called a Parks vector. Applying this concept to the generalized six pulse inverter of figure. 1. It can be seen that

of the eight possible output voltage states two are null voltage vectors. Remaining six voltage vectors are each spatially displaced  $60^\circ$  apart as depicted in figure 2(a) (where the H and L nomenclature refers to the output being switched High (+VDC) or Low C-VDC, respectively). The space vector PWM generation technique involves



equating volt-second intervals between a desired reference voltage vector and the output voltage vectors realizable by the six pulse bridge inverter.

Figure 1: Generalized schematic for a six pulse bridge inverter

For example, the reference voltage vector shown in Figure 2(a) may be generated by using the immediately adjacent inverter Output voltage vectors to provide the required phase displacement while the null voltage vectors  $U_0$  and  $U_7$  control the magnitude. In this implementation a typical modulation cycle consists of the following sequence of switching states (labelled 1 to 8 in figure 2): from which an equation equating the volt-second integrals of these switching states with that of us is given as:

$$U_9.T = u_0.Q + U_a.t_a + U_b.t_b + U_7.t_7$$

$$\text{Where } T = t_0 + t_a + t_b + t_7$$

As can be seen from figure 2 the vectorial decomposition of  $U_s$  in figure 2 is essentially equivalent to the triangulation method timing diagram figure.2 (b). For the traditional space vector technique to is chosen equal to  $t_7$  and the waveforms are then a special case of the triangulation technique with a modified reference waveform, formed by the addition of an

essentially triangular, third harmonic distortion waveform to the desired sinusoidal component as shown in figure. 3 Due to the inherent additive third harmonic triangle waveform, the characteristics of the space vector PWM waveforms are very similar to those obtained through the addition of third harmonic sinusoidal distortion to a triangulation modulator although, as will be shown later, the space vector generation technique presented in this paper has many advantages over the traditional triangulation method - in particular it is more amenable to microprocessor implementation.

torque/inertia and power/weight ratios, high speed, low maintenance, small size, low weight and cost, and high efficiency over low and high speed ranges. Permanent magnet motors and induction motors have most of the mentioned features. Permanent magnet motors have an advantage over the induction motor from the point view of operation efficiency, but these motors are more expensive and it is not easy to perform field weakening in order to increase the range of speed with such motors. Moreover, this type of machine presents recycling difficulties. This can be a big problem when these motors are used in large scale in electrical cars. On the other hand, the induction motors are less expensive, easily recyclable and requires less maintenance. For this project the motor needs a totally enclosed construction in order to protect it from external environment. The overloading possibility is limited at 30% of motor rated torque because the cooling efficiency is limited by the enclosed construction of the motor. In table I the induction motor characteristics are shown. The propulsion system consists of a single motor driving there are wheels via a fixed ratio gearbox and differential.

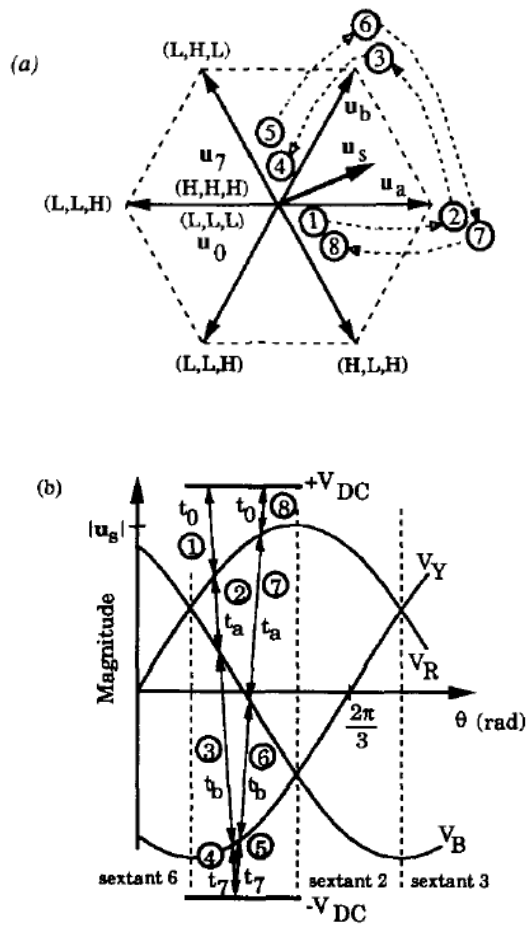


Figure 2: A single PWM modulation cycle (stages I to 8) consixed from:  
 (a) space vector method,  $U_S = f(u_a, u_t)$ .  
 (b) triangulation method using inter section points.

III. MOTOR DETAILS

In general the desired features of the motor for an electric vehicle are high

TABLE I. Induction motor characteristics

S.No.	Functions	Ranges
1.	Rated Power	1.1KW
2.	Rated Torque	7.7 Nm
3.	Maximum Torque	18.6 Nm
4.	Rated Speed	1400 rpm
5.	Rated Frequency	50Hz
6.	Voltage	70V
7.	Rated Current	16A
8.	Weight	11Kg

IV. CONTROL CIRCUIT

Power semiconductor switches over the last decade have been paralleled by increasing inverter switching frequencies which in turn necessitate the use of more efficient PWM waveform synthesis

techniques. While ultrasonic switching frequencies are largely the domain of hysteretic type modulation strategies, the majority of digital PWM modulators are implemented using low cost microprocessors or application specific integrated circuits computing the 8WM switching times in real-time up to but a few kHz.

The impetus for the development of a new microprocessor based PWM generation algorithm was to reduce time spent computing the PWM switching times originally performed using the triangulation technique in order to allow more time for actually controlling; the motor. Figure. 3 details an existing modulator hardware structure, based on the methods described in and the corresponding PWM pulse timing format used to define a single PWM cycle.

Computing the PWM switching points using the triangulation technique involves evaluating three sets of  $T_1$  and  $T_2$  times defining three PWM pulses, as illustrated in figures 3(b), and this requires the following (interrupt level) microprocessor operations: Lookups, 6 Multiplies, 12 Subtractions and 6 checks on the  $T_1$  and  $T_2$  times to account for the generation of unrealizable times. This scheme, implemented with the hardware of figure 3(a), takes typically 750 to compute and to download the PWM switching times to the AMD9513 timer so that, for a 1 KHz switching rate only 25% of the microprocessor time is left for actual controlling the motor. The proposed space vector generation strategy is based around the simple proportioning of a modulation time  $T_m$ , which is equal to the "active" time  $t_a + t_b$  of the PWM waveform as shown in figure 3(b). If  $T_m$  is held constant the resulting voltage vector traces out a hexagonal locus (trapezoidal phase voltage) as illustrated in figure 3(b). In this case the times  $t_a$  and  $t_b$  can simply be obtained by essentially linearly proportioning  $T_m$  based on the intersect and angle  $\alpha$  where  $\alpha$  varies over the range 0 to  $n/3$  within a particular sextant, and is related to  $\epsilon$  by an offset angle comprised of a constant  $n/6$  displacement and an integer number of

$n/3$  sextant widths. This procedure is computationally efficient although in order to obtain a sinusoidal phase voltage (circular voltage vector trajectory) the magnitude of the  $V_{ref}$ . reference hexagon must be dynamically scaled as a function of  $\alpha$ .

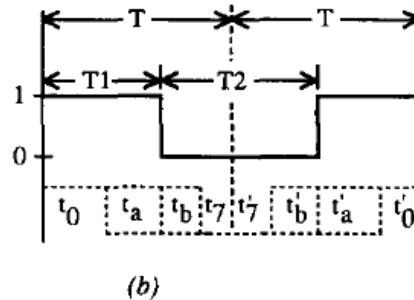
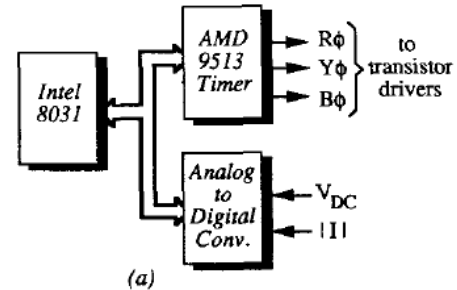


Figure 3 (a) Typical Microprocessor PWM Hardware. (b) PWM Pulse timing format for 9513 in terms of  $T_1$  and  $T_2$  compared with times  $t_0, t_a, t_b$  and  $t_7$ .

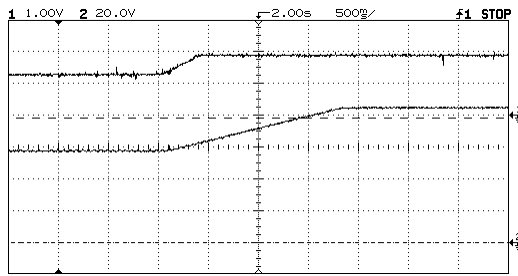
### V.SIMULATION RESULT

The control system of figure.4 is implemented on the laboratory induction motor drives using a digital controller board. Extensive tests have been carried out to confirm the validity and reliability of the proposed low cost control unit.

An experimental set-up has been used for the tests in the laboratory before the ones carried out with the chassis. It consists of a test bench (with a programmable powder brake, an incremental encoder and a tachometer generator, and a torque sensor, all from Leroy Somer) and the dSPACE development system, ACE Kit 1103, based on the DS1103 PPC controller board, the

Real-Time Interface(RTI) block set for Simulink as well as experiment software (Control Desk, MLIB/MTRACE).

Tests with Different Speed Commands



(a)

Figure 4 (a) shows the result when a step command of about 47 rad/s is set at 6 s, where the speed change from 103 rad/s to 150 rad/s.

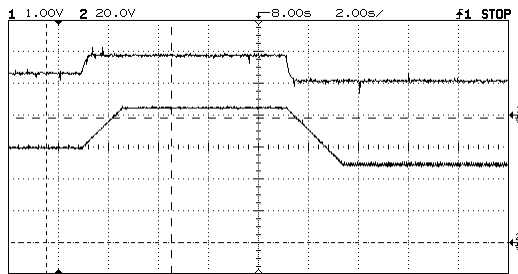


figure 4(b) is shown the response of a variation in the speed reference from 105 rad/s to 150 rad/s, and then to 87 rad/s.

These experiments are performed in order to analyse the performance of the control unit to step variation in speed reference and also to investigate the system behaviour with step increase and decrease of the speed. We can see a good speed build up and very stable performance.

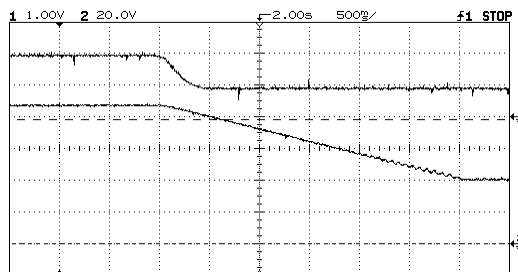


Figure. 4(c) shows another test with reduction in the speed reference from about 154 rad/sto 71 rad/s.

VI. OPERATION AND WORKING

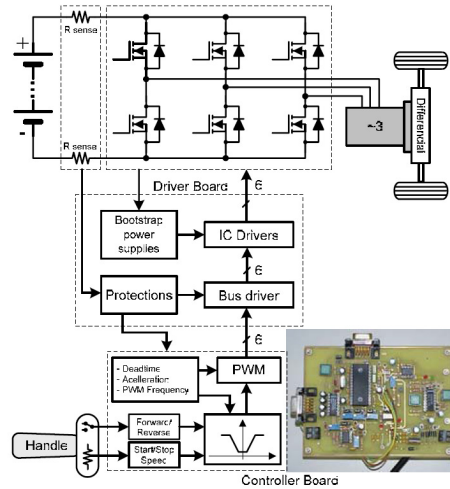


Figure.5. Hardware circuit diagram

The main subsystems implemented are: generating circuit, voltage/frequency law, PWM modulator, driver circuits and power inverter. The most universally accepted motor drive topology is used, that consists of a six-switch voltage inverter driving a three-phase induction motor as shown in figure 5. The voltage inverter is built by means of six power MOSFETs, ref. IRFP 260N, from International Rectifier. Their drain source breakdown voltage is 200V, and the maximum drain current is 46A (at 25° C). The DC bus voltage will vary from 96 V to 108 V, depending on the charge state of the batteries. A 200V device would allow adequate margin above inductive di/dt voltage spikes. The MOSFETs continuous current rating is determined by power loss. Typically if a sine wave of current has a peak of 22,6 A, the current rating of the device should be 45,2 A. Peak currents up to 46 A would be suitable so long as maximum junction temperature does not exceed 150° C. Others topics of circuit design that require same attention are: gate drive, physical bus structure and protection circuits. The gate drive is an important element of the inverter



design. The implementation of a power supply for the high side circuitry in half-bridge inverter is problematic because the high side power supply is connected to the switching output of the half-bridge. In the driver board the bootstrap circuits are used to generate the floating power supplies for the high side circuitry of half bridge inverters. These circuits provide a simple, low cost, and effective method of generating floating voltage supplies. Considering the high di/dt of the MOSFETs, it is important to minimize stray inductance. The circuit inverter implements a low inductance DC bus by laminating together positive and negative bus bars to take advantage of flux cancelling. The power board has been designed to support current protections. This is achieved by means of two shunt resistors placed on DC bus. The basic circuit was implemented as shown in figure. 5, using the high speed opto coupler HCPL2611. Figure. 5 shows the response of the protection circuit during a fault detection. The signal of channel 1 corresponds to the output of the opto coupler HCPL2611, in the circuit of figure. 5 and the signal of channel 2 corresponds to the one of the PWM inputs of the drive HCPL314J, in the circuit of fig. 3. The respective delay is less than 200 ns and the overall delay since the over voltage detected in the resistances Sense until the gates of the MOSFETs is less than 200 ns plus the propagation delay of the HCPL2611 and HCPL314J which is less than 0.7 $\mu$ s.

## VII. CONCLUSION

In this project the design of a three-wheeled electric scooter has been presented. The scalar control method is a simple and inexpensive method for induction motor control, implemented on a low cost digital controller board. The experimental results show that the implementation of the space vector control strategy on a digital platform based on a microcontroller is feasible and reliable in this kind of application concerning an electric scooter. The aim of this project was to demonstrate that light electric scooters could be a viable alternative to traditional scooters powered by internal

combustion engines (two or four stroke). The prototype realization has been carried out successfully and the experimental results have shown that the controller performs a stable and efficient motor control, without penalizing performances of the conventional scooter.

## REFERENCES

1. Amirjan Bin Nawabjan (2009). *Automated attendance management software*. University of Technology, Malaysia: Degree Thesis.
2. Pathan, RFID Based Toll Deduction System, I.J. Information Technology and Computer Science, 2012, 4, 40-46 Published Online April 2012 in MECS.
3. Billard .F.Cookes (2001). *Fundamentals on barcode technology*. Cyprus: Rafot Press Lilimited.
4. Emenike .U. Ugwuatu (2007). *Future of RFID technology in Nigeria*. Ibadan: Loyato Press.
5. Joshué Pérez , Fernando Seco, Vicente Milanés, Antonio Jiménez, Julio C. Díaz and Teresa de Pedro, An RFID-Based Intelligent Vehicle Speed Controller Using Active Traffic Signals, Sensors 2010, 10, 5872-5887.
6. Lovemore Gunda, Lee Masuka, Reginald Gonye, Samson Mhlanga and Lungile Nyang RFID based automatic tollgate system (RATS), CIE42 Proceedings, 16-18 July 2012, Cape Town, South Africa 2012 CIE & SAIIE.
7. Ononiwu G. Chiagozie, Okorafor G. Nwaji, Radio frequency identification (rfid) based attendance system with automatic door unit, Academic Research International, ISSN-L: 2223-9553, ISSN: 2223-9944 Vol. 2, No. 2, March 2014.

